Paper publicar[1] **/ *Published paper*:**

Aragüés-Peñalba, M., Egea Álvarez, A., Galceran Arellano, S. and Gomis Bellmunt, O. (2015) Optimal power flow tool for mixed highvoltage alternating current and high-voltage direct current systems for grid integration of large wind power plants. IET Electric Power Applications, 9. 8. 876-881. Doi: 10.1049/iet-rpg.2015.0028

[1] Substituir per la citació bibliogràfica corresponent

IET Renewable Power Generation

Research Article

Optimal power flow tool for mixed high-voltage alternating current and high-voltage direct current systems for grid integration of large wind power plants

ISSN 1752-1416
Received on 30th January 2015
Revised on 22nd June 2015
Accepted on 7th July 2015
doi: 10.1049/iet-rpg.2015.0028
www.ietdl.org

Mònica Aragüés-Peñalba[1] ✉, Agustí Egea Alvarez[1], Samuel Galceran Arellano[1], Oriol Gomis-Bellmunt[1,2]

[1]*CITCEA-UPC, Electrical Engineering Department, Technical University of Catalonia, Diagonal 647 Planta 2, Barcelona, Spain*
[2]*Catalonia Institute for Energy Research, Electrical Engineering Area, IREC, Jardins de Dones de Negre 1, 08963 Sant Adrià del Besòs, Barcelona, Spain*
✉ *E-mail: monica.aragues@citcea.upc.edu*

Abstract: This study presents a tool for solving optimal power flows (OPFs) in hybrid high-voltage direct current (HVDC) and high-voltage alternating current (HVAC) systems for grid integration of large wind power plants, located either offshore or onshore. The OPF departs from the assumption that the power being produced from the wind power plants is known, as well as the demand from the AC grid. To model the interaction between the DC and AC grids, the active power conservation is expressed between the AC side and DC side of each converter, taking into consideration converter losses (modelled as a second-order polynomial). The tool developed determines the voltages and the active and reactive power in each bus and branch that ensure the selected objective function. All the electrical variables are limited. Moreover, the currents flowing in each DC and AC branch are also limited. The maximum AC voltage that can be applied by the converters is also limited. To develop the tool, both HVDC and HVAC grids need to be represented appropriately through its impedances and admittances. The tool has been implemented through MATLAB® optimisation toolbox and through a more specific optimisation software GAMS®, leading to the same results for the study case presented.

1 Introduction

The progress in power electronics, as well as the improvement of cables performance have favoured and still stimulate the development of high-voltage direct current (HVDC) technology, in parallel with high-voltage alternating current (HVAC). The choice of a technology or the other one will depend, to begin with, on the technical feasibility of each one for the specific link to be constructed [1]. Two examples of this large dependence on the technical requirements can be advanced. If the electrical connection to be constructed links two systems working at different frequency (asynchronous systems), HVDC must be used. With HVDC the power transmitted is practically independent of the distance, whereas, in HVAC the power capability transmission decreases with distance. However, the larger expenses of HVDC installations for certain distances compared with the HVAC option (around 50–80 km for submarine or underground transmissions and around 600–800 km for overhead transmission) can favour the HVAC construction. Taking into consideration the before mentioned, a scenario for transmission networks based on interconnections between HVDC and HVAC grids is feasible and seems probable [2]. Specially, if HVDC technology is used for delivering the power produced in the wind power plants to the terrestrial grid. Thinking in remote wind power plants to be connected to different AC grids, then the HVDC system could be multiterminal [3–8].

An optimal power flow (OPF) for operating HVDC multiterminal grids was proposed and compared with droop control in [9]. The present study enlarges the OPF for mixed HVDC–HVAC systems. Although many studies exist focusing on the operation of AC grids and DC grids separately, only a few have been published analysing the operation of AC and DC grids combined. In [10], an algorithm for solving power flows in AC/DC networks is presented and implemented in MATPOWER®, taking into account converter losses through a generalised converter loss model proposed in [11]. The optimal operation of hybrid AC/DC systems is addressed in the studies [12–16]. In the first study listed [12], some power system elements are represented with limited accuracy: terminal VSC losses are neglected and only point-to-point connections are defined. Converter losses are included in [13–16]. Baradar [13] focused on the mathematical formulation of the problem, which is non-convex. The problem is reformulated for AC grids with embedded DC networks based on second-order cone programming, which converts it into a convex problem. However, the optimal operation is only addressed in terms of loss minimisation. Similarly, Cao *et al.* [14] only deal with transmission losses. However, it is worth mentioning that [14] takes into consideration additional constraints to include grid code requirements, neglected in other studies.

In [15, 16], different optimisation goals are addressed. They define and optimise, for different objective functions, DC and AC load flows simultaneously in a random AC–DC network, allowing the possibility of meshing the DC system. The work in [15] was implemented through MATLAB® optimisation toolbox and [16] was implemented in MATPOWER®, modifying the code and solver so as to add easily non-linear constraints and define cost functions. Although DC and AC links are combined, the effect of a scenario with large wind power penetration transmitted through the DC grids is not evaluated in any of them.

The proposed tool here has been applied to a scenario where the HVDC system would enable the transmission of a large amount of wind power, providing a sensitivity analysis of the effect of wind power variation in the objective function analysed. It was implemented first in MATLAB® optimisation toolbox (function *fmincon*) and it was benchmarked with [16], leading to the same results for a particular study case and for two different objective functions, in [17], so it was validated. Secondly, it was implemented in GAMS®, reducing the computation time significantly compared with the MATLAB implementation. The fact that it was implemented in an optimisation dedicated software, allows the choice among multiple solvers and guarantees fast computations, which is essential for dealing with large networks. The OPF results enable a comparison of the losses in the different system components: DC and AC cables/lines, converters and transformers, for different wind power plant injections. The analysis of a particular study shows that the results of the OPF can help in an operational perspective.

This paper is organised as follows. The mathematical formulation of the tool is first presented in Section 2. Then, the tool is applied to a six DC, eight AC bus network for loss minimisation in Section 3. The results obtained with MATLAB® and GAMS® coincide. Therefore, the tool has been validated, offering a flexible methodology for analysing hybrid AC/DC grids optimal operation.

2 Optimisation problem

The optimisation problem involves DC and AC power systems and can be thus considered as a non-linear constrained optimisation type. Mainly two strategies can be used to solve DC and AC power flows: sequential and unified. The sequential approach ([11, 18]) separates the problem in two parts corresponding each one to DC and AC power flow equations, respectively. Unified approach [13] solves all the equations together. The OPF tool presented here is based on a unified strategy. Several objective functions can be defined for the optimisation tool. An interesting one that will be shown through a case study is the overall Joule losses in the HVDC–HVAC network.

The layout of a general HVDC–HVAC system to which the tool is applied is shown in Fig. 1. The converter topology is voltage source converter (VSC), allowing an independent control of active and reactive power. The VSC connected to the wind farms (wind farm rectifiers) inject the wind power to the HVDC grid. In normal operational mode, the wind farm rectifiers absorb all the power produced and inject it into the DC grid while supplying the reactive power needed to maintain the AC wind farm voltage. The power in the DC network is injected to the AC grid through grid-connected VSC, responsible for the HVDC grid voltage control and which provide reactive power support to the AC grid when needed. The AC grid is constituted by AC links [overhead lines (OHL) or underground cables], forming a mesh, that allow the electrical power to be transmitted to the consumption nodes.

The active power on the AC side and DC side of the converter differ on losses. Hence, the AC power can be defined as a function of the DC power and converter losses, modelled according to a second-order polynomial of the AC converter current. DC cables are modelled through their resistances, AC cables are represented according to their π equivalent and transformers are modelled as an equivalent impedance with inductive and resistive part.

The active and reactive power demands in the AC nodes and the injections from the wind power plants are an input for the tool. The electrical characteristics of the DC and AC grids, as well as of lines and cables and the converter loss parameters are also known data. The tool determines the active and reactive power injections (or absorptions) from generators and converters and the power flowing through each branch that minimise a specified objective function while accomplishing the electrical system constraints.

2.1 Notation

All the variables and parameters required for the mathematical formulation of the problem are listed below.

$\boldsymbol{G}_{\mathrm{DC}}$ is the conductance matrix of the DC grid
$\boldsymbol{G}_{\mathrm{AC}}$ is the conductance matrix of the AC grid
$\boldsymbol{B}_{\mathrm{AC}}$ susceptance matrix of the AC grid
$i \in (1, n)$, n is the number of VSC converters
$j \in (1, p)$, p is the number of AC nodes
$\boldsymbol{I} = [I_1 \cdots I_n]^{\mathrm{T}}$ is the vector of DC currents
$\boldsymbol{E} = [E_1 \cdots E_n]^{\mathrm{T}}$ is the vector of DC voltages
$\boldsymbol{V} = [V_1 \cdots V_p]^{\mathrm{T}}$ is the vector of AC voltage magnitude
$\boldsymbol{\delta} = [\delta_1 \cdots \delta_p]^{\mathrm{T}}$ is the vector of AC voltage angles
E_i and I_i are, respectively, the DC voltage and the current in node i.
V_j and δ_j are, respectively, the AC voltage magnitude and angle of voltage phasor in node j
$\boldsymbol{P}_{\mathrm{DC}} = \left[P_{\mathrm{DC}_1} \ldots P_{\mathrm{DC}_n}\right]^{\mathrm{T}}$ is the power entering the DC system through the converters
$\boldsymbol{P}_{\mathrm{g}} = \left[P_{\mathrm{g}_1} \ldots P_{\mathrm{g}_p}\right]^{\mathrm{T}}$ is the active power generated in each AC node
$\boldsymbol{P}_{\mathrm{d}} = \left[P_{\mathrm{d}_1} \ldots P_{\mathrm{d}_p}\right]^{\mathrm{T}}$ is the active power demanded in each AC node
$\boldsymbol{Q}_{\mathrm{vsc}} = [Q_1 \ldots Q_n]^{\mathrm{T}}$ is the reactive power injection/absorption by each converter

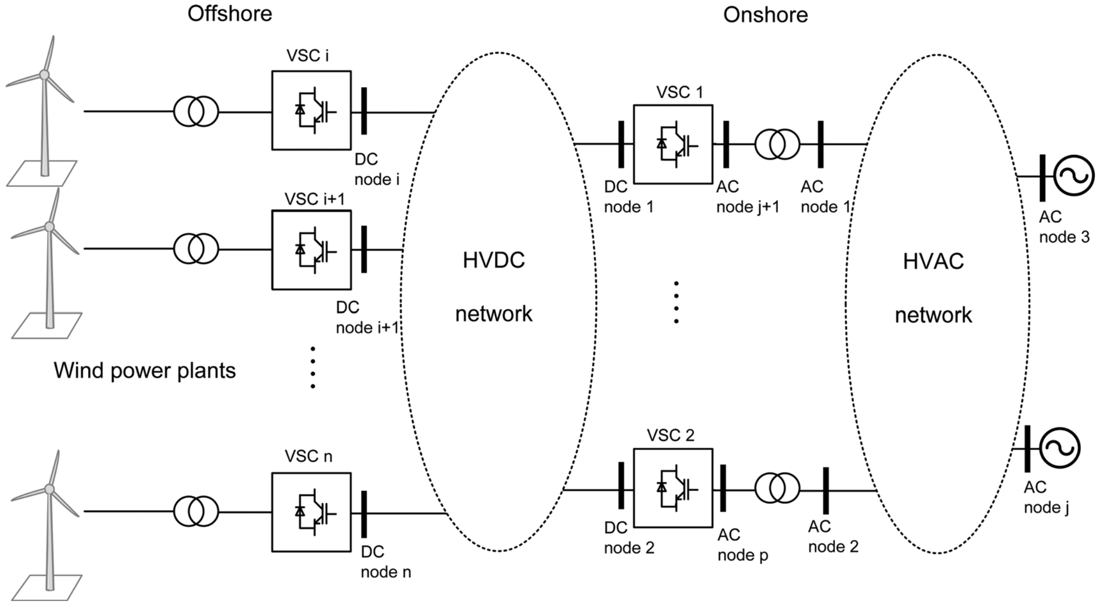

Fig. 1 *Hybrid HVDC–HVAC system for integrating offshore wind power*

IET Renew. Power Gener., pp. 1–6

$\boldsymbol{Q}_g = \left[Q_{g_1} \dots Q_{g_p}\right]^T$ is the reactive power generated in each AC node
$\boldsymbol{Q}_d = \left[Q_{d_1} \dots Q_{d_p}\right]^T$ is the reactive power demanded in each AC node
$\boldsymbol{S}_{vsc} = [S_1 \dots S_n]^T$ is the power rating of each converter

2.2 Inputs

The input data for the optimisation problem is listed below.

- Conductance matrix of the DC grid: $\boldsymbol{G}_{DC}$
- Conductance and susceptance matrix of the AC grid: $\boldsymbol{G}_{AC}$ and $\boldsymbol{B}_{AC}$
- Active and reactive power demand in the AC grid nodes: $\boldsymbol{P}_d$ and $\boldsymbol{Q}_d$
- Converter loss parameters

2.3 Outputs

The optimisation algorithm determines the voltages in all the nodes and the power flowing in the different branches of the system that minimise a user defined objective function and guarantee all the equality and inequality constraints. Therefore, the output vector of the algorithm, $\boldsymbol{x}$, contains the following information:

$$\boldsymbol{x} = \begin{bmatrix} E \\ I \\ V \\ \delta \\ P \\ Q \end{bmatrix} \quad (1)$$

2.4 Mathematical formulation

The problem is formulated here taking a general objective function, $f(x)$, which is dependent on the variables defined in (1).

$$[\text{MIN}] z = f(x) \quad (2)$$

subject to the following constraints:

$$\boldsymbol{I} = \boldsymbol{G}_{DC}\boldsymbol{E} \quad (3)$$

$$P_{DC_i} = E_i I_i \quad (4)$$

$$P_{DC_i} - P_{lossvsc_i} = P_j + P_{g_j} - P_{d_j} \quad (5)$$

$$Q_j = Q_{vsc_j} + Q_{g_j} - Q_{d_j} \quad (6)$$

$$E_i^{min} \le E_i \le E_i^{max} \quad (7)$$

$$I_i^{min} \le I_i \le I_i^{max} \quad (8)$$

$$P_{kl}^{min} \le G_{kl}(E_k - E_l)E_k \le P_{kl}^{max} \quad (9)$$

$$V_j^{min} \le V_j \le V_j^{max} \quad (10)$$

$$P_j^{min} \le P_j \le P_j^{max} \quad (11)$$

$$Q_j^{min} \le Q_j \le Q_j^{max} \quad (12)$$

$$S_{kl}^{min} \le S_{kl} \le S_{kl}^{max} \quad (13)$$

$$\delta_j^{min} \le \delta_j \le \delta_j^{max} \quad (14)$$

$$S_{vsc_i}^{min} \le \boldsymbol{S}_{vsc} \le S_{vsc_i}^{max} \quad (15)$$

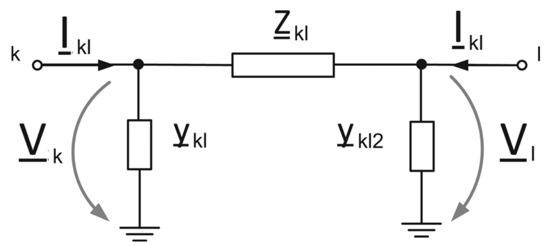

Fig. 2 *π equivalent of the AC branch between nodes k and l*

being

$$P_j = V_j \sum_{k=1}^{p} V_k \left(G_{AC_{jk}} \cos\delta_{jk} + B_{AC_{jk}} \sin\delta_{jk}\right) \quad (16)$$

$$Q_j = V_j \sum_{k=1}^{p} V_k \left(G_{AC_{jk}} \sin\delta_{jk} - B_{AC_{jk}} \cos\delta_{jk}\right) \quad (17)$$

The AC links are modelled according to the π equivalent diagram, as sketched in Fig. 2.

2.5 Converter model

The converter topology chosen for this study is VSC, allowing and independent control of active and reactive power. The active power exchange on the AC and DC side of the converter differ on losses. Hence, the AC power can be defined as a function of the DC power and converter losses, modelled according to a second-order polynomial, as in [11]

$$P_{lossvsc_i} = a + bI_{vsc_i} + cI_{vsc_i}^2 \quad (18)$$

where a, b and c are p.u. parameters given by Table 1 and I_{vsc_i} represents the p.u. current flowing through the converter i

$$I_{vsc_i}^* = \frac{\sqrt{P_{vsc_i}^2 + Q_{vsc_i}^2}}{V_i} \quad (19)$$

As reflected in Table 1, two operating modes are distinguished for VSCs: rectifier and inverter.

2.6 Objective functions

The objective function presented in (2) can be chosen among several functions which are of interest in terms of operation or planning of the system. Some of them are listed below.

Minimum power losses (to be applied in systems or subsystems where the total transmission losses want to be minimised):

$$[\text{MIN}] z = \sum_{j=1}^{p} \left(P_{g_j} - P_{d_j}\right) \quad (20)$$

Minimum generation costs (to be applied when the cost function of generation of the different generating units is known and depends on the power delivered; the production of units with minimum

Table 1 Converter loss parameters [11]

VSC	*a*	*b*	*c*
rectifier	11.033×10^{-3}	3.464×10^{-3}	5.40×10^{-3}
inverter	11.033×10^{-3}	3.464×10^{-3}	7.67×10^{-3}

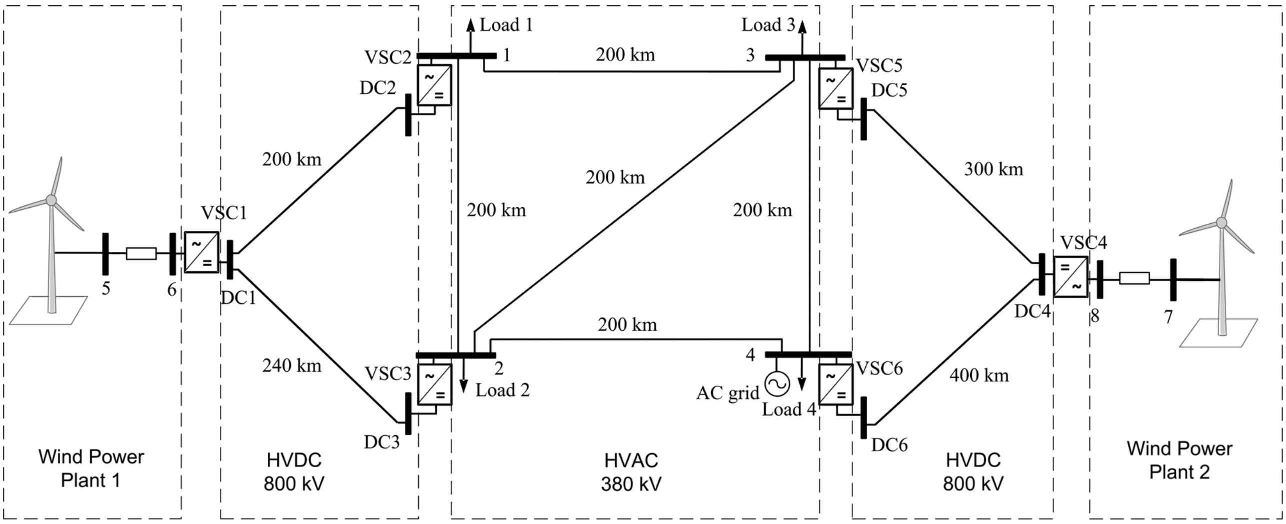

Fig. 3 *Power system analysed*

generating cost will be prioritised):

$$[\text{MIN}]z = \sum_{j=1}^{n_g} C_j(P_{g_j}) \tag{21}$$

where n_g represents the number of generators.

Maximum reactive power margin (to be applied when some generators have to deliver maximum reactive power support):

$$[\text{MAX}]z = \sum_{j=1}^{n_g} Q_{g_j} \tag{22}$$

where n_g represents the number of generators.

Bus voltages closest to a profile (to be applied when certain buses need to keep their voltage at a specific value or the closest possible to it):

$$[\text{MIN}]z = \sum_{j=1}^{p} \left(V_j - V_{\text{set}}\right)^2 \tag{23}$$

Minimum deviation from another state (to be applied when a specific magnitude wants to be kept at a specific value or the closest possible to it):

$$[\text{MIN}]z = \sum_{j=1}^{p} \left(x_j - x_{\text{set}}\right)^2 \tag{24}$$

3 System under study

The system used for this study is a six DC bus and eight AC bus network, based on the test system defined by CIGRÈ in [19] and sketched in Fig. 3. Basically two DC systems, consisting of three buses each, allow to export and distribute the power generated by two wind power plants. Their internal AC grid and step-up transformer are modelled through an equivalent impedance. The power produced is then transmitted to a six bus AC system to reach the loads. The DC and AC systems are linked through six VSC converters. The AC system, where all the branches are OHL, is rated to 380 kV and the DC system voltage, where all the branches are cables, has a voltage level of ±400 kV. Their electrical parameters are specified in Table 2. The wind farm VSCs are rated to 1000 MVA. The user needs to specify the control variables of the system (e.g. the generators injections and voltages setpoints).

Table 2 Electrical parameters of the AC and DC branches

Branch type	Resistance, Ω/km	Inductance, mH/km	Capacitance, μF/km
DC cable ±400 kV	0.0095	2.1120	0.1906
AC OHL 380 kV	0.0200	0.8532	0.0135

The active and reactive power demand (loads) is defined by vectors $\boldsymbol{P}_d$ and $\boldsymbol{Q}_d$ in MW and MVar, respectively. Their values for the eight AC nodes of this study case are represented in Table 3.

3.1 Minimum losses

This section shows the results of the optimisation problem obtained when minimising losses in the hybrid DC/AC system sketched in Fig. 3. The minimum losses of the whole system, computed as the difference between total active generation and total demand (20) are 12.705 MW in MATLAB® and 12.712 MW in GAMS®. The DC and AC voltages on the different buses are reflected in Tables 4 and 5. Although there is some difference after the third

Table 3 Active and reactive power demand in the AC nodes

Demand	1	2	3	4	5	6	7	8
$\boldsymbol{P}_d$, MW	400	600	800	400	0	0	0	0
$\boldsymbol{Q}_d$, MVar	50	50	50	20	0	0	0	0

Table 4 Bus voltages for loss minimisation in MATLAB®

Bus	AC voltage magnitude, p.u.	AC voltage angle, rad	DC voltage of VSC
1	0.998	−0.059	1.099
2	1.000	−0.019	1.098
3	0.997	−0.064	1.097
4	1.000	0	1.099
5	1.099	0.006	–
6	1.098	−0.006	1.098
7	1.099	0.006	–
8	1.098	−0.006	1.099

Table 5 Bus voltages for loss minimisation in GAMS®

Bus	AC voltage magnitude, p.u	AC voltage angle, rad	DC voltage of VSC
1	0.998	–0.059	1.099
2	1.000	–0.018	1.098
3	0.997	–0.064	1.099
4	1.000	0	1.099
5	1.100	0	–
6	1.099	–0.012	1.100
7	1.100	0	–
8	1.099	–0.012	1.100

decimal, it can be concluded that both softwares lead to the same operating point. The active and reactive power flows are shown in Fig. 4.

It is worth mentioning that the computation time of GAMS® for the presented study case is 0.087 s using solver CONOPT and 0.069 s using solver IPOPT, while it takes 8 s in MATLAB® *fmincon* with interior point algorithm using a barrier function [20] as solver. Table 6 shows that GAMS® keeps low computation time values for larger grids. In MATLAB® *fmincon* the execution time rises faster with the number of buses (and thus, variables). Hence, GAMS not only allows fast computation times, but is also prepared to deal with larger problems.

The first solver used in GAMS is CONOPT. CONOPT is designed for large and sparse models and it removes from the model recursive equations and variables. It has a fast method for finding a first feasible solution, especially interesting for models with few degrees of freedom. It is very appropriate for models with approximately the same number of constraints as variables. It is thought for models with smooth functions, but it can also be applied to models that do not have differentiable functions [21]. To evaluate the effectiveness of other GAMS® solvers for non-linear programming (and to check that the low computation time is not only a matter of the solver but also thanks to the mathematical pre-treatment of this software) another solver has been tried. If the number of variables is much larger than the number of constraints, CONOPT and IPOPT will use second derivatives, but their methodology is different and it is not easy to predict which solver will be more appropriate.

Table 6 Execution time of GAMS for different power system sizes

Solver	8 AC 6 DC	12 AC 6 DC	20 AC 6 DC	70 AC 6 DC
CONOPT execution time, s	0.087	0.121	0.150	0.228
IPOPT execution time, s	0.069	0.070	0.126	0.288

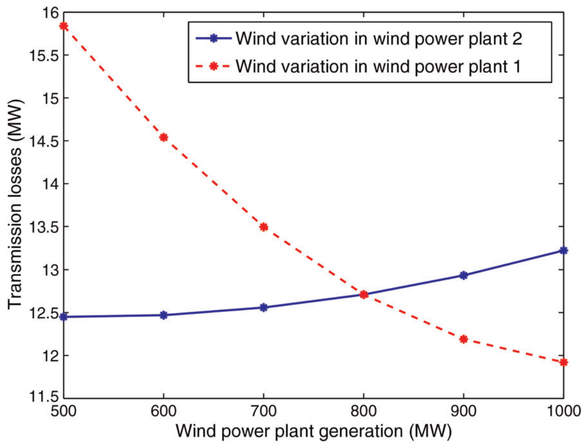

Fig. 5 *Effect of wind power variation on the objective function*

3.2 Sensitivity to wind speed changes

The variation of wind speed in any of the two wind power plants changes the power flows distribution and affects the objective function value. A variation of the wind power injected from each wind power plant has been evaluated keeping the other wind power plant generation, as depicted in Fig. 5. The active and reactive power demands are assumed to be the same as that in Section 3.1. Hence, while in the before mentioned study case both wind power plants were producing 800 MW, if the one connected to bus 5 (wind power plant 1) increases its production in 10%, the total transmission losses turn to be 11.92 MW (lower). In case this wind power plant decreases its production in 10%, the transmission losses are 14.54 MW (higher). Hence, if the wind power generation increases in wind power plant 1, the total transmission losses decrease.

However, the effect of wind power variation of the wind power plant connected to bus 7 (wind power plant 2) on the objective function is in the opposite sense: if the generation increases, the transmission losses also increase. The main explanation is that the DC grid to which wind power plant 2 is connected presents longer distance and therefore losses, compared with the DC grid to which wind power plant 1 is connected.

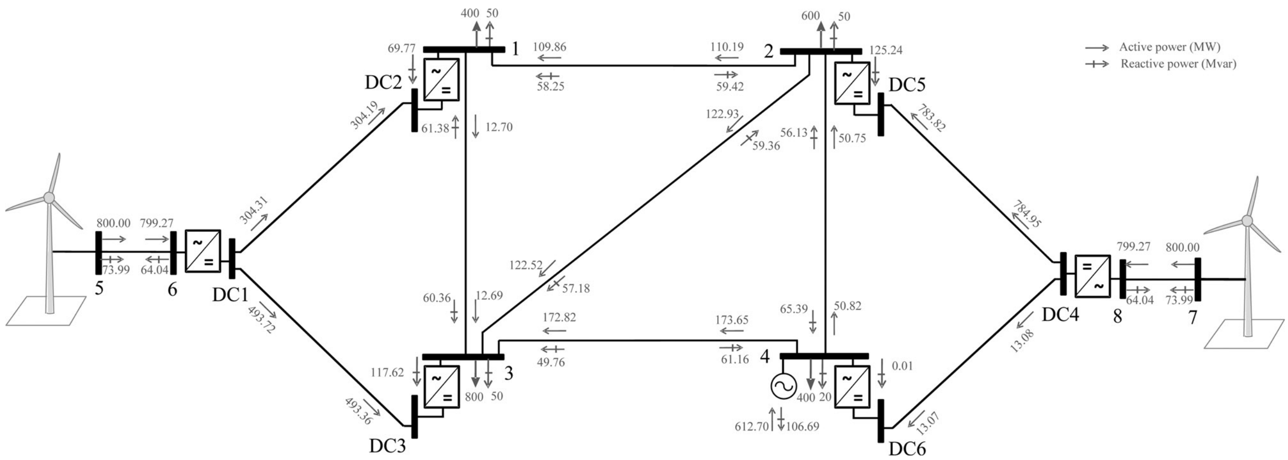

Fig. 4 *Power flows for loss minimisation*

4 Conclusions

This paper presents an OPF strategy to operate hybrid DC/AC systems with large penetration of offshore wind. This methodology was already benchmarked with [16], obtaining the same results for two study cases analysed in [17]. The tool has been applied to a particular study case consisting in a two DC grids connected to an AC grid. Two softwares have been used for its implementation (MATLAB® and GAMS®) leading to the same results for the study case of loss minimisation presented. However, GAMS®, for being an optimisation dedicated software, has been proved to be far more efficient than MATLAB® *fmincon*. Hence, the tool represents a fast, flexible and validated methodology for analysing the optimal operation of hybrid AC/DC grids with large wind power integration for several objective functions.

5 Acknowledgments

This work was supported by the Ministerio de Ciencia de Innovación under the projects ENE2012-33043 and ENE2013-47296 and by EIT KIC InnoEnergy project Smart Power.

6 References

1 Bahrman, M.P., Johnson, B.K.: 'The ABCs of HVDC transmission technologies', *IEEE Power Energy Mag.*, 2007, **5**, (2), pp. 32–44

2 CIGRÉ Working Group B-4.52: 'HVDC grid feasibility study'. International Council for Large Electric Systems (CIGRÉ), Technical Brochure 533, 2013

3 Gomis-Bellmunt, O., Liang, J., Ekanayake, J., *et al.*: 'Topologies of multiterminal HVDC-VSC transmission for large offshore wind farms', *Electr. Power Syst. Res.*, 2011, **81**, (2), pp. 271–281

4 Van Hertem, D., Ghandhari, M.: 'Multi-terminal VSC HVDC for the European supergrid: obstacles', *Renew. Sust. Energy Rev.*, 2010, **14**, (9), pp. 3156–3163

5 Egea-Alvarez, A., Beerten, J., Van Hertem, D., *et al.*: 'Primary and secondary power control of multiterminal HVDC grids'. Tenth IET Int. Conf. on AC and DC Power Transmission (ACDC 2012), 2012, pp. 1–6

6 Aragüés-Peñalba, M., Egea-Àlvarez, A., Gomis-Bellmunt, O., *et al.*: 'Optimum voltage control for loss minimization in HVDC multi-terminal transmission systems for large offshore wind farms', *Electr. Power Syst. Res.*, 2012, **89**, pp. 54–63

7 Prieto-Araujo, E., Bianchi, F.D., Junyent-Ferre, A., *et al.*: 'Methodology for droop control dynamic analysis of multiterminal VSC-HVDC grids for offshore wind farms', *IEEE Trans. Power Deliv.*, 2011, **26**, (4), pp. 2476–2485

8 Egea-Alvarez, A., Daniel Bianchi, F., Junyent-Ferré, A., *et al.*: 'Voltage control of multiterminal VSC-HVDC transmission systems for offshore wind power plants: design and implementation in a scaled platform', *IEEE Trans. Ind. Electron.*, 2013, **60**, (6), pp. 2381–2391

9 Aragüés-Peñalba, M., Egea-Alvarez, A., Gomis-Bellmunt, O., *et al.*: 'Optimum voltage control for loss minimization in HVDC multi-terminal transmission systems for large offshore wind farms', *Electr. Power Syst. Res.*, 2012, **89**, pp. 54–63

10 Beerten, J., Cole, S., Belmans, R.: 'A sequential AC/DC power flow algorithm for networks containing multi-terminal VSC HVDC systems', IEEE Power and Energy Society General Meeting, 2010, 2010, pp. 1–7

11 Beerten, J., Cole, S., Belmans, R.: 'Generalized steady state VSC MTDC model for sequential AC/DC power flow algorithms', *IEEE Trans. Power Syst.*, 2012, **27**, (2), pp. 821–829

12 Pizano-Martinez, A., Fuerte-Esquivel, C.R., Ambriz-Perez, H., *et al.*: 'Modeling of VSC-based HVDC systems for a Newton–Raphson OPF algorithm', *IEEE Trans. Power Syst.*, 2007, **22**, (4), pp. 1794–1803

13 Baradar, M.: 'Modeling of multi terminal HVDC systems in power flow and optimal power flow formulations'. Licenciate thesis, KTH Royal Institute of Technology, Stockholm, Sweden, 2013

14 Cao, J., Wenjuan, D., Wang, H.F., *et al.*: 'Minimization of transmission loss in meshed ac/dc grids with VSC-MTDC networks', *IEEE Trans. Power Syst.*, 2013, **28**, (3), pp. 3047–3055

15 Wiget, R., Andersson, G.: 'Optimal power flow for combined ac and multi-terminal HVDC grids based on VSC converters', IEEE Power and Energy Society General Meeting, 2012, 2012, pp. 1–8

16 Rimez, J., Belmans, R.: 'A combined AC/DC optimal power flow algorithm for meshed AC and DC networks linked by VSC converters', *Int. Trans. Electr. Energy Syst.*, 2014, http://dx.doi.org/10.1002/etep.1943

17 Aragüés-Peñalba, M., Beerten, J., Rimez, J., *et al.*: 'Optimal power flow tool for hybrid dc/ac systems', AC and DC Power Transmission, 11th IET International Conference on, Birmingham, 2014, pp. 1–7

18 Messalti, S., Saadate, S.B., Flieller, D.S.: 'A new approach for load flow analysis of integrated AC/DC power systems using sequential modified Gauss-Seidel methods', *Eur. Trans. Electr. Power*, 2012, **22**, pp. 421–432

19 CIGRÉ Working Groups B4–58 (devices for load flow control and methodologies for direct voltage control in a meshed HVDC grid) and B4–57 (guide for the development of models for HVDC converters in a HVDC grid). The CIGRÉ B4 DC grid test system. International Council for Large Electric Systems (CIGRÉ), 2013

20 Byrd, R.H., Gilbert, J.: 'A trust region method based on interior point techniques for nonlinear programming', *Math. Program.*, 1996, **89**, pp. 149–185

21 GAMS: 'The solver manuals' (GAMS Development Corporation, Washington, DC, USA, 2015)